Implementation of the immersed boundary method for solving problems of fluid dynamics with moving bodies

Implementation of the immersed boundary method for solving problems of fluid dynamics with moving bodies

S A Filimonov[1,2], A A Gavrilov[1,2] and A A Dekterev[1,2]

[1]Kutateladze Institute of Thermophysics SB RAS, Lavrenteva av. 1, 630090, Novosibirsk, Russia
[2]Siberian Federal University, Svobodniy 79/10, 660041, Krasnoyarsk, Russia

Abstract. This paper presents the implementation of the immersed boundary method (IBM) for grids consisting of arbitrary cells. This approach allows to combine the IBM with the body-fitted method (BFM). The implementation is based on the combination of the "ghost-cell" method and penalization method. The paper presents the IBM to determine the basic design parameters and the results of the verification of the method for laminar and turbulent flow regimes for both Newtonian and viscoplastic fluids. In the last test, the method was used to simulate a flow in an annular channel with the orbital motion of the inner cylinder.

1. Introduction

The immersed boundaries method (IBM) allows to spend less time to prepare the numerical model and it requires fewer grid cells for bodies of complex shapes than the body-fitted method (BF). The disadvantages of the IBM include a significant number of additional operations required to determine the calculated geometric parameters; however, this approach effective to simulate the flow of a moving body.

When the IBM is applied a solid body is “immersed” in the existing computational grid, and divides the grid into several subdomains – 1) the area of the liquid, 2) the area of the body, and 3) the boundary of the body. In the cells that intersect the boundary of the body a volume force which leads the liquid velocity in the cell to the velocity of the body boundary is introduced. The IBM was first proposed by Peskin in 1972 to simulate flow around a heart valve in Cartesian coordinates [1]. The essence of the proposed method is to combine the Eulerian and Langrangian approaches: turbulent fluid flow is described by a system of Reynolds equations on a fixed Cartesian grid, and the movable "submerged" boundary is given in the form of massless Langrangian points. The interaction between the wall boundaries and the flow is given as a volume force in the momentum conservation equation, which is given as a δ-function of the distance from the center of the Euler cell to the Langrangian point. Works [2–4] present a review of IBM and fluid-structure interaction.

The immersed boundary method is mostly used for Cartesian grids, but in our research, the IBM for grids with arbitrary cells is implemented. This approach will allow the BF method (fixed body or channel wall of a complex shape) with IBM (moving body). In our version of the method, we used a combined approach of the “ghost-cell” method [5] and the penalization method.

2. Methodology

2.1. Governing equations

The simulation of a viscous incompressible flow is described by the Navier-Stokes equations:

$$\nabla(\rho\mathbf{v}) = 0, \tag{1}$$

$$\frac{\partial(\rho\mathbf{v})}{\partial t} + \rho(\mathbf{v}\cdot\nabla)\mathbf{v} = -\nabla p + \nabla\boldsymbol{\tau} + \mathbf{f} \tag{2}$$

where $\mathbf{v}$ is the velocity vector, ρ is the density, p is the pressure, and τ is the total stress tensor, $\mathbf{f}$ is the force acting on the border and inside the body, which leads the velocity of the fluid to the speed of the border. The turbulent characteristics are determined by two-equation $k-\omega$ SST model by Menter [6].

2.2. Body motion definition

The rigid body is determined by a closed surface. The body can move in space at a linear speed $\mathbf{v}_{lin}$, and also rotate around a given center with angular velocity $\boldsymbol{\omega}$. Thus, the speed $\mathbf{v}_s$ of a point of the body is determined by the following equation:

$$\mathbf{v}_s = \boldsymbol{\omega}\times\mathbf{r}_s + \mathbf{v}_{lin}, \tag{3}$$

where $\mathbf{r}_s$ is the radius vector from the point to the center of rotation.

2.3. Definition of the interaction force.

To define $\mathbf{f}$, we use the combination of the "ghosts-cell" method and the penalization method. The immersed boundary divides all cells into three groups (figure 1): 1) cells that are completely outside the body, where $\mathbf{f} \equiv 0$; 2) cells that are completely inside the body, where $\mathbf{f} = \mathbf{f}_{iner}$, 3) cells that are crossed by the border where, $\mathbf{f} = \mathbf{f}_{bound}$.

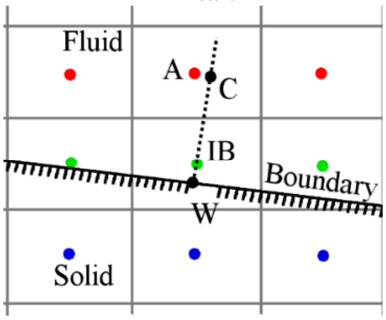

Figure 1. The division of the calculation domain by an immersed boundary.

$$\mathbf{f}_{bound} = \rho\frac{\mathbf{v}_{IB} - \mathbf{v}_{liq}}{\Delta t}\chi \tag{4}$$

where $\mathbf{v}_{liq}$ is the velocity value in the cell obtained by solving the momentum conservation equation, Δt is the time step, χ is the penalization parameter, $\mathbf{v}_{IB}$ is the velocity in the cell IB as shown in figure 1, which is determined by the interpolation between points C and W. The penalization parameter has to be specified in the simulation, which could be beneficial since with proper tuning accuracy could be improved. However, the parameter should not be too large, it can had to a linear system with a very large stiffness. The Positions of points C and W are defined by the following approach. Point W is the projection of point IB on the boundary. Point C lies in a neighboring cell (A) on a straight line which goes through points W and IB. The velocity value at point C is determined as follows:

$$\mathbf{v}_C = \mathbf{v}_A + \nabla\mathbf{v}\cdot\mathrm{d}\mathbf{r} \tag{5}$$

where $\mathbf{v}_A$ is the velocity in point A, $\nabla\mathbf{v}$ is the gradient velocity in the cell, $\mathrm{d}\mathbf{r} = \mathbf{r}_C - \mathbf{r}_A$ is the distance from A to C. The linear interpolation is suitable for laminar and low Reynolds flow conditions [7]:

$$\mathbf{v}_{\mathrm{IB}} = \frac{(\mathbf{v}_{\mathrm{C}} - \mathbf{v}_{\mathrm{W}})h_1}{h_2} + \mathbf{v}_{\mathrm{W}} \tag{6}$$

where h_1 is the distance between W and IB, h_2 is the distance between W and C. It should be noted that point IB can be located both outside the solid body and inside it; in this case, h_1 is taken with a negative sign. Value $\mathbf{v}_{\mathrm{W}}$ is determined by the equation (3). The force acting on the inner cell $\mathbf{f}_{inner}$ is calculated same $\mathbf{f}_{bound}$ with the difference $\mathbf{v}_{IB} = \mathbf{v}_s$. The specific dissipation of the kinetic energy of turbulence is set for the version of a low-Reynolds model of the turbulence at point IB:

$$\omega = \frac{6 \cdot \mu}{C_\beta \cdot \rho \cdot y_n^2}, \tag{7}$$

where μ is the molecular viscosity, C_β is constant 0.075, $y_n = h_2/2$. The turbulent parameters in the cells that are inside the body are equal to null.

3. Testing

The IBM was vivificated follow tests: test 1 – non-stationary laminar flow past a two-dimensional cylinder; test 2 – turbulent flow in a channel with a backward step; test 3 – fluid flow in an annular channel, with a rotating inner cylinder; 4) test 4 – fluid flow in an annular channel, with orbital motion of the inner cylinder. For the first and second tests, a comparison will be made with the experimental data and the calculation data obtained by the BFM method. For the third one only with the calculations data obtained by the BFM, and fourth with the calculations dataobtained by other researchers.

3.1. Non-stationary laminar flow around a two-dimensional cylinder.

Two-dimensional unsteady flow around a cylinder was simulated. The Reynolds number was set to 100. Instant velocity magnitude is shown in figure 2.

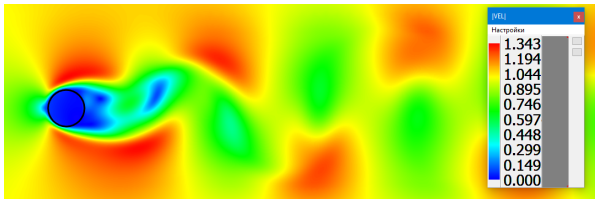

Figure 2. Velocity magnitude.

The calculations show the vortex shedding frequency deviates from the experimental data [8, 9] at about $St < 2\%$. The time averaged drag coefficient coincide the experimental date with an accuracy about $C_D < 4\%$. The evolution of the forces acting on the cylinder over time is shown in figure 3.

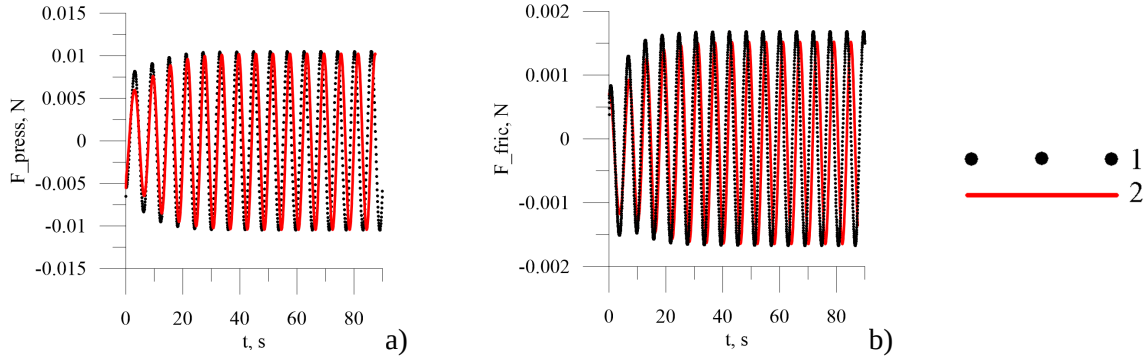

Figure 3. The time dependence of the pressure and friction forces acting on the cylinder: a) the transverse pressure component; b) transverse friction component. 1 – BFM, 2– IBM.

3.2. The flow of a non-Newtonian fluid in the annular channel, with a rotating inner cylinder

The most advantageous use of the method of immersed boundaries is simulation of moving bodies. An example of such a problem is the calculation of the drill string rotation in a well. The flow of a non-Newtonian fluid in an annular channel with a rotating inner cylinder is considered. For Herschel–Bulkley fluid, the effective viscosity is determined by the ratio:

$$\mu = \left(\tau_0 + k_v \dot{\gamma}^n\right) / \dot{\gamma} \tag{8}$$

where τ_0 is a yield stress $\dot{\gamma}$ is the mean shear rate, k_v is the consistency parameter, and n is the power-law index. The algorithm for calculating the steady-state flow of viscoplastic fluids in the annular channel is described in [11]. Two versions of the 2D model BFM and IBM with the ratio of the diameters of the inner and outer cylinder $k = 0.5$ and eccentricity $\varepsilon = 0.5$ was built. The grid in the cross section was constructed using the octo-tree method (see figure 4). Three grids consisting of 12000, 36000 and 120000 cells were later built. The pressure drop deviation between BFM and IBM for the three options of grids was 6%, 2% and 1%, respectively. The flow rate was based on the axial Reynolds number $\mathrm{Re} = 344$ and the angular velocity of rotation was set for the value of the Taylor number $\mathrm{Ta} = 8100$. Figure 4 presents the fields of axial velocity and effective viscosity for the two variants of the test.

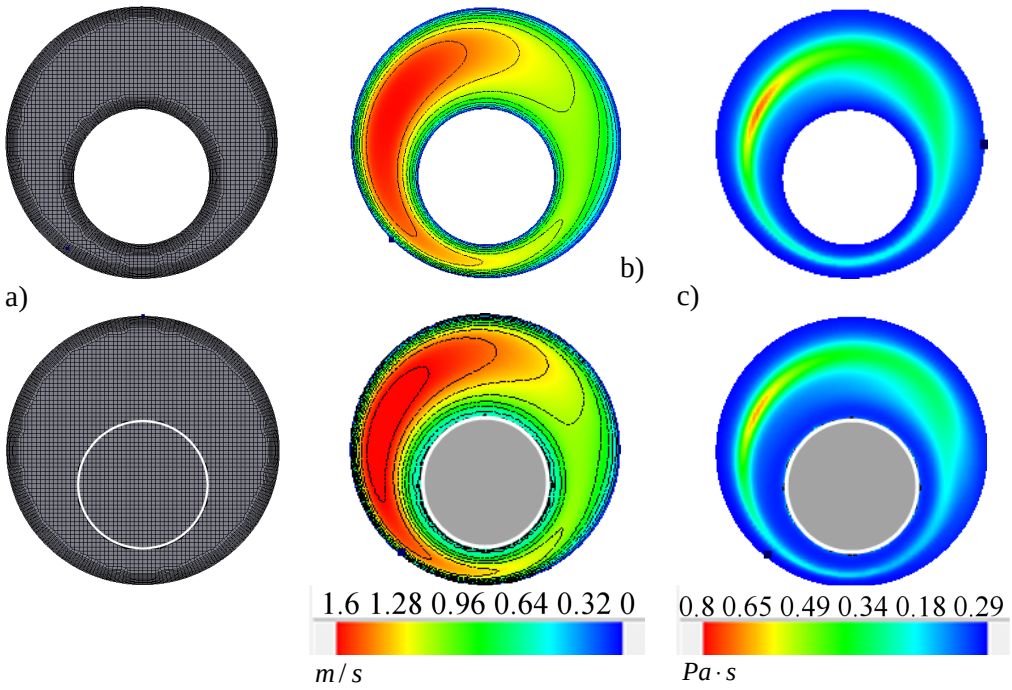

Figure 4. a) Computational grid; b) axial velocity; c) viscosity fields for BFM (above), IBM (below).

3.3. Simulation of the flow in an annular channel with orbital motion of the inner cylinder

A more complex type of movement of the inner cylinder is the combination of rotation around its own axis with angular velocity ω and orbital motion around the center of the outer cylinder with angular velocity Ω (see figure 5). A series of calculations was carried out for different ratios of the angular velocities of the internal cylinder with Newtonian fluid. The geometry of the test is the same as in the previous test.

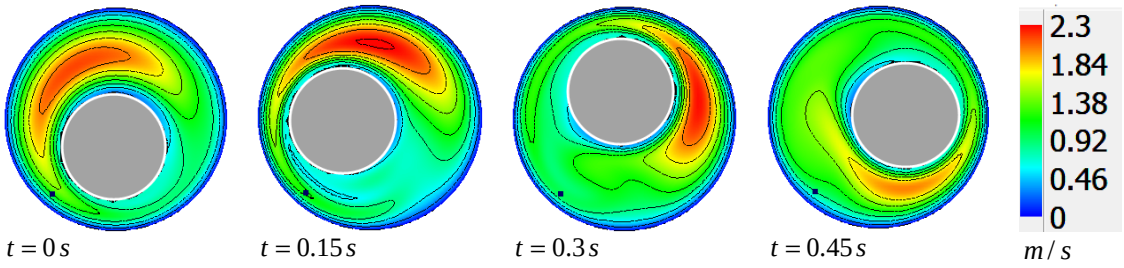

Figure 5. Instant distribution of the velocity vector magnitude in the annular channel at different time instances.

The ratio of the velocities was set by the ratio of the Reynolds number relative to the orbital motion and the Reynolds number relative to the rotation of the inner cylinder around its own axis:

$$\lambda = \mathrm{Re}_O / \mathrm{Re}_I ;\ \mathrm{Re}_O = \rho \cdot \Omega \cdot \delta^2 / \mu ;\ \mathrm{Re}_I = \rho \cdot \omega \cdot Ri^2 / \mu , \qquad (9, 10, 11)$$

where δ is the mean annular gap ($R_O - R_I$) the difference between the radii of the outer and inner cylinder), μ is the dynamic viscosity, R_I is the inner cylinder radius, R_O is the outer cylinder radius. The calculation results were compared with the results were obtained by Feng[12], which are obtained in a rotating reference frame. Comparison was made by means of dimensionless forces Fx, Fy where Fx is the force directed along the radius of the orbital motion to the center of rotation, Fy is the force directed tangentially to the path of the inner cylinder center,

$$Fx = \frac{\left(F_x^p + F_x^s\right)}{\rho\left(\omega \cdot Ri\right)^2 \delta \cdot \Delta z}; \qquad Fy = \frac{\left(F_y^p + F_y^s\right)}{\rho\left(\omega \cdot Ri\right)^2 \delta \cdot \Delta z} \qquad (12)$$

where $F_x^p, F_y^p, F_x^s, F_y^s$ are the projections of pressure and friction forces on the corresponding direction, $\rho\left(\omega \cdot Ri\right)^2 \delta \cdot \Delta z$ is the dimensionless complex, Δz is the length of the channel. The calculation results are shown in figure 6. They show that with increasing λ, radial and tangential forces monotonously increase. Radial force Fx at small λ has a centrifugal direction, and vice versa, it has centripetal direction with large λ. The similar situation is with tangential force Fy – at $\lambda < 0.2$ the forces acting on the inner cylinder coincide with the orbital rotation direction, and vice versa.

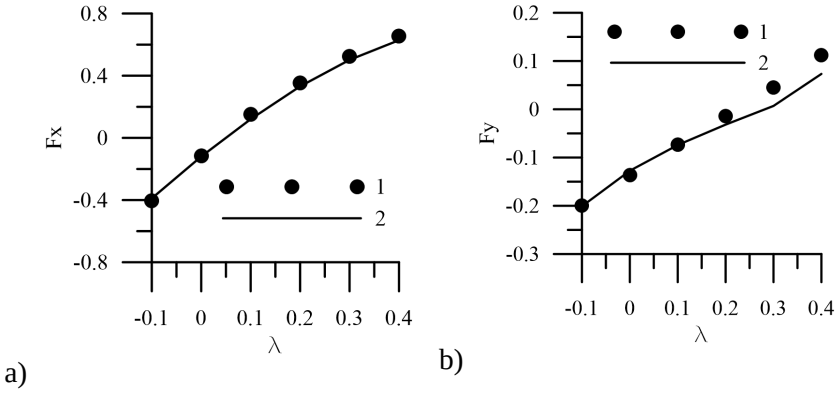

Figure 6. The value of the radial Fx and tangential Fy forces relative to the orbital motion 1 – feng, 2 – calculation.

Conclusion

The numerical method of immersed boundaries has been implemented, which makes it possible to effectively method the interaction of a fluid with a complex rheology and a body moving in it. The test results show good agreement with the experimental data an the results obtained in other modeling methods. Further development of the method will be aimed at modeling a two-phase medium.

Acknowledgments

This work was carried out under state contract with IT SB RAS (AAAA-A17-117030910025-7).

Reference

[1] Peskin C S 1972 *J. Comput. Phys.* **10** 252–71
[2] Mittal R and Iaccarino G 2005 *Fluid Mech* **37** 239–61
[3] Bandringa H 2010 *Immersed boundary methods* (Netherlands: University of Groningen)
[4] Kim W and Choi H 2019 *Int. J. Heat Fluid Flow* **75** 301–9
[5] Mohd-Yosuf J 1997 *Annu. Res. Briefs* 317–28
[6] Menter F R 1993 *AIAA Pap* **2906**
[7] Roman F, Armenio V and Fröhlich J 2009 *Phys. Fluids* **21** 101701
[8] Tritton D J 1959 *J. Fluid Mech.* **6** 547
[9] Zdravkovich M M 1997 *Flow around circular cylinders, vol 1: Fundamentals* (Oxford: Oxford University Press)
[10] Dellenback P A, Metzger D E, and Neitzel G P 1988 *AIAA J.* **26** 669–81
[11] Gavrilov A A, Minakov A V, Dekterev A A, and Rudyak V YA 2012 *Vychislitel'nyye tekhnologii* **12** 44–56
[12] Feng S, Li Q, and Fu S 2007 *Int. J. Numer. Methods Fluids* **54** 2 155–73